NANO LETTERS

2006
Vol. 6, No. 2
277−281

Magic Structures of H-Passivated ⟨110⟩ Silicon Nanowires

Tzu-Liang Chan

US Department of Energy Ames Laboratory and Physics Department, Iowa State University, Ames, Iowa 50011

Cristian V. Ciobanu*

Division of Engineering, Colorado School of Mines, Golden, Colorado 80401

Feng-Chuan Chuang, Ning Lu, Cai-Zhuang Wang, and Kai-Ming Ho

US Department of Energy Ames Laboratory and Physics Department, Iowa State University, Ames, Iowa 50011

Received November 15, 2005

ABSTRACT

We report a genetic algorithm approach combined with ab initio calculations to determine the structure of hydrogenated ⟨110⟩ Si nanowires. As the number of atoms per length increases, we find that the cross section of the nanowire evolves from chains of six-atom rings to fused pairs of such chains to hexagons bounded by {001} and {111} facets. Our calculations predict that hexagonal wires become stable starting at about 1.2 nm diameter, which is consistent with recent experimental reports of nanowires with diameters of about 3 nm.

The continuous miniaturization in the electronics industry has reached the limit in which the interconnection of the devices in a reliable and controllable way is particularly challenging. Fervent strides are underway in the preparation of nanoscale wires for molecular and nanoelectronics applications:[1] such wires (possibly doped or functionalized) can operate both as nanoscale devices and as interconnects.[2] Silicon nanowires (SiNW) offer, in addition to their appeal as building blocks for nanoscale electronics, the benefit of simple fabrication techniques compatible with the currently well-developed silicon technology.

The current growth methods (e.g., refs 3−6) can yield wires with diameters ranging from several tens of nanometers down to 1 nm. These SiNWs are usually crystalline with only a few axis orientations observed and have a prismatic shape bounded by facets that are parallel to the wire axis.[4−8] While remarkable progress has been achieved in terms of preparation and characterization of SiNWs, atomic-level knowledge of the structure remains necessary for a complete understanding the device properties of these wires. At present, attempts to predict the structure of SiNWs are affected by the lack of robust methodologies (i.e., algorithms coupled with model interactions) for searching the configuration space, and most studies to date rely on heuristically proposed structures as the starting point for stability studies of SiNWs at the ab initio level. Electronic structure calculations are too computationally demanding to be used in a thorough sampling of the potential energy surface of SiNWs. On the other hand, most of the empirical potentials for Si are fast but are not sufficiently transferable to capture accurately the structure and energetics of various wire configurations. Despite these obstacles, the current theoretical efforts to find the structure of SiNWs have been very vigorous and have lead to the identification of a number of low-energy configurations for pristine SiNWs.[9−13] In comparison, the structure of passivated nanowires has received much less attention from a theoretical perspective, although most of the experimental techniques to date yield wires that are passivated either with oxides[14,15] or with hydrogen.[6,7]

Motivated by the scanning tunneling microscopy (STM) experiments of Ma et al.,[6] we have investigated the structure of thin H-passivated nanowires oriented along the [110] direction. To this end, we have designed a robust and efficient optimization procedure based on a genetic algorithm (GA), followed by structural refinements at the density functional theory (DFT) level. We have found that in the presence of hydrogen, the silicon atoms of the nanowire can maintain their bulklike bonding environment down to subnanometer wire dimensions. Furthermore, our calculations reveal that, as the number of atoms per length is increased,

* Corresponding author: e-mail, cciobanu@mines.edu; phone, 303-384-2119; fax, 303-273-3602.

10.1021/nl0522633 CCC: $33.50
Published on Web 01/11/2006

there emerge three distinct types of wire configurations with low formation energies (magic wires). Two of these structures have a platelike aspect in cross section, which have not been observed so far. The third one has a hexagonal section, which is consistent with recent experiments for Si and Ge wires.[6,16] Given their extremely small diameters, the magic structures found here by the combined GA-DFT optimization procedure cannot be predicted by thermodynamic considerations based on the Wulff construction.[17] The procedure described below is generally applicable for finding the structure of any ultrathin nanowire provided that suitable models for the atomic interactions are available and that the spatial periodicity along the wire axis is known.

The choice of GA for the present work was motivated by previous findings that search procedures inspired by the genetic evolution can successfully be used to determine the structure of Si clusters[18] and surfaces.[19,20] The SiNW are modeled using a supercell that is periodic in one dimension, with the period set according to experiments.[6] We choose the Hansel−Vogel (HV) potential to describe the atomic interactions, for this model has been shown to reproduce well the energies of hydrogenated phases of the Si(001) surface.[21]

The algorithm for SiNW optimization is similar to that which we recently designed for high-index Si surfaces,[19] so we focus here on the departures from ref 19. During a GA optimization run, a pool of at least 60 structures (which are initially just random collections of atoms) is evolved by performing mating operations; such operations consist in selecting two random structures (parents) from the pool, cutting them with the same plane parallel to the wire axis, and then combining parts of the parent structures that lie on the opposite sides on the cutting plane to create a new structure (child).[19] The child structure is passivated by satisfying all its dangling bonds with H atoms and then relaxed with the HV model.[21] We include the child structure in the genetic pool based on its formation energy f defined as

$$f = (E - \mu_H n_H)/n - \mu \quad (1)$$

where E is the total energy of the computational cell with n silicon atoms (n is kept fixed during a GA run) and n_H hydrogen atoms, μ is the (reference) bulk cohesive energy of Si in its diamond structure, and μ_H is the chemical potential of hydrogen. The H chemical potential is set such that certain hydrogenation reactions at surfaces are thermodynamically possible. These reactions are shown in Figure 1a, along with our two chosen values for μ_H. The pool is divided into two equal subsets, one for each value of μ_H. The mating operations are performed both with parents in the same subset and with parents in different subsets, to ensure a superior sampling of the potential energy landscape. The mating is carried out 15 times during a generation, and a typical GA run has 50 000 generations. At the end of each run, all structures are relaxed using the VASP package.[22,23] The chemical potential μ_H used to compute DFT formation energies is determined so that it maximizes the correlation with the HV formation energies for a few hundred configurations (refer to Figure 1b). Therefore, while some energetic reordering does occur after the DFT calculations, most of the low-energy structures found with the HV model remain relevant at the DFT level, especially in the range of DFT formation energies below 0.15 eV/per atom.

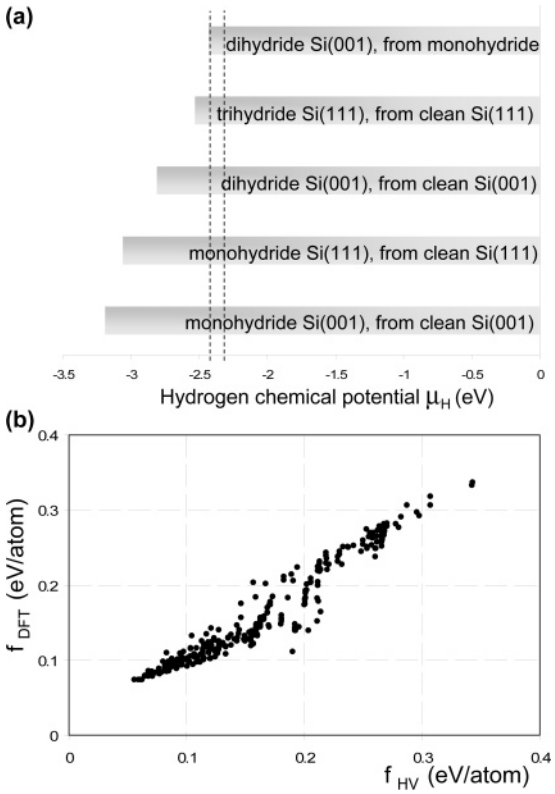

Figure 1. (a) Choice of the chemical potential μ_H used in the genetic algorithm search with the HV potential. The vertical lines are located at $\mu_H = -2.42$ eV and $\mu_H = -2.32$ eV. Each horizontal bar shows the μ_H range for which a given hydrogenation reaction is favorable. (b) Formation energy f_{DFT} at the DFT level[22] versus the same quantity computed with the HV model[21] at $\mu_H = -2.42$ eV. The chemical potential $\mu_H = -3.45$ eV for the DFT calculations was determined so as to maximize the correlation between the DFT and HV formation energies for 422 structures (data points). The magic wires described in the paper lie below 0.15 eV, where the agreement between the DFT and the HV values is best.

The most stable structures (DFT level) that we found through the above procedure using $\mu_H = -3.45$ eV are shown in Figure 2 for different numbers of Si atoms in the range $10 \le n \le 30$. The second half of the genetic pool (corresponding to $\mu_H = -3.35$ eV (DFT)) retrieved the same structures for all even values of n. In the case of odd n, the two sides of the pool found structures that are different only in the position of one peripheral Si atom. As Figure 2 reveals, the GA-DFT optimization finds stable structures that are made of six-atom rings (viewed along the SiNW axis), with some of the rings incomplete depending on the value of n. The six rings can arrange themselves in chains (e.g., $n = 12$, $n = 16$ in Figure 2); for $n > 16$ the rings form fused pairs of such chains ($n = 18$, 24, 30), which we call double chains. Structures similar to the double chains shown in Figure 2 have also been considered in recent studies of quantum confinement in SiNWs.[25] The formation energy of the most stable structures for $10 \le n \le 30$ retrieved is plotted

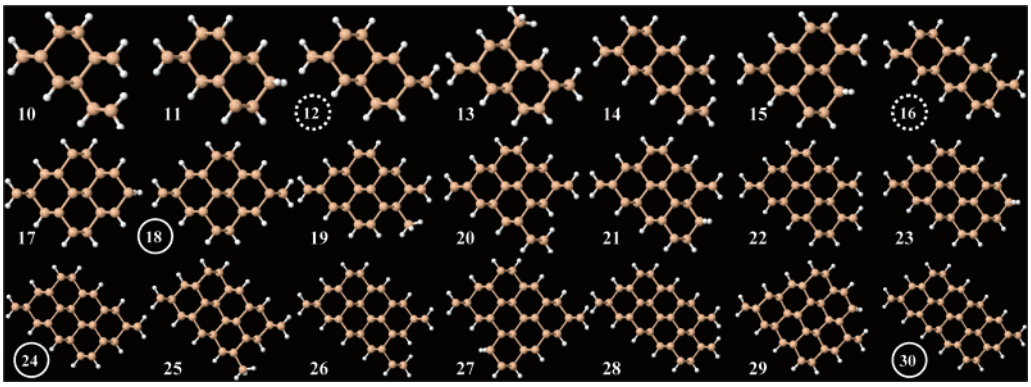

Figure 2. Nanowire structures (axial view) with $n = 10$ to $n = 30$ silicon atoms per unit cell, found after genetic algorithm optimizations and the subsequent DFT relaxations. The H atoms are the smaller white spheres. The values n that correspond to magic wires are indicated by dashed and solid circles for chain and double-chain SiNWs, respectively.

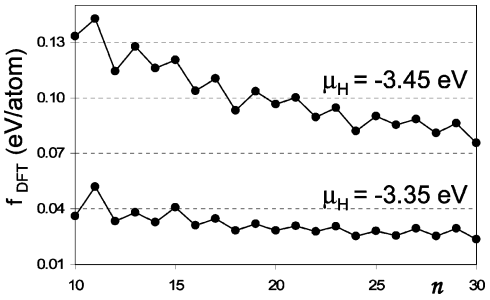

Figure 3. DFT formation energies per Si atom for two values of the H chemical potential, plotted as a function of n. Structures with even n are local minima at *both* the empirical[21] and ab initio[22] levels.

in Figure 3 as a function of n. When the value of n increases, the formation energy assumes an overall decreasing trend while displaying odd−even oscillations. The relatively larger formation energy of the odd-n structures corresponds to configurations where one Si atom protrudes from the surface of the wires, thus creating a somewhat unfavorable bonding environment.

As shown in Figure 2, the ground state for each n has a bulklike structure with no significant reconstructions. The absence of reconstruction is due to the hydrogen environment at chemical potentials μ_H that favor no less than five hydrogenation reactions (refer to Figure 1). The use of smaller μ_H values can lead to understanding the interplay between reconstruction and hydrogen coverage on the SiNW facets, an investigation which we will address in subsequent studies. For smaller values of n ($n < 17$), the common motif present in lowest energy structures is the six-atom ring. When chains of complete six-atoms rings are formed, the structures become particularly stable, as is the case of $n = 12$ and $n = 16$ SiNWs, which are made of $R = 2$ and $R = 3$ complete rings, respectively. The six-atom ring chains expose two {111} facets with monohydride terminations. Another common feature of all (complete) chain structures is the presence of two dihydridres with the SiH_2 planes oriented perpendicular to the wire axis. For $n > 17$, the most favorable structures are the double chains described above (and illustrated in Figure 2), whose building blocks we call double rings. These blocks are readily identifiable in the case of $n = 18$, 24, and 30, which correspond to a number of $D = 2$, 3, and 4 full double rings (respectively). The double chains expose a total of four {111} nanofacets which form parallelogram-shaped SiNW cross sections. The complete double chains also contain two dihydrides, identical to those capping the chain SiNWs.

We have conducted further optimization studies for $n > 30$ using, however, only even atom numbers n. We found that starting at $n = 60$, structures with hexagonal cross section becomes stable over the double-chain SiNWs described above. Even the smallest hexagonal SiNW ($n = 28$) has a formation energy that is only slightly higher (by 0.005 eV/atom) than that of the double chain with the nearest size ($n = 30$). The hexagonal wires are bounded by two {001} and four {111} facets and can be described by their number of completed concentric layers L of six-atom rings. Due to the relative stability and structural closure of the chain, double-chain, and hexagonal SiNWs, we name these configurations *magic*. The shapes of prototype magic SiNWs are illustrated in Figure 4, and a description of their building blocks and numbers of atoms is summarized in Table 1. The formation energies of magic SiNWs were separately plotted as a function of n in Figure 5 at both levels of theory.[21,22] The plot reflects the structural trends described above, namely, the transition between chain and double chain at $n = 16$ and the transition between double-chain and hexagonal SiNWs, which starts at $n \sim 29$. It should be noted that *incomplete* hexagons appear frequently in the range $28 < n < 60$; therefore the latter shape transition is not as well defined as the former.

We note that even in the absence of reconstruction, the shape of SiNWs (refer to Figure 4) departs markedly from the equilibrium crystal shape predicted by the constrained minimization[17] of the overall surface energy. The reason for this departure is that the number of surface Si atoms is larger than, or comparable to, the number of bulklike atoms (refer to Table 1). For the chain and double-chain SiNWs, the polygonal shape itself is not preserved as only two or four facets are exposed instead of the expected six.[6,7] For the ultrathin hexagonal wires, the departure from the Wulff construction[17] is more subtle. Although the cross section is hexagonal, the relative size of the {100} and {111} facets

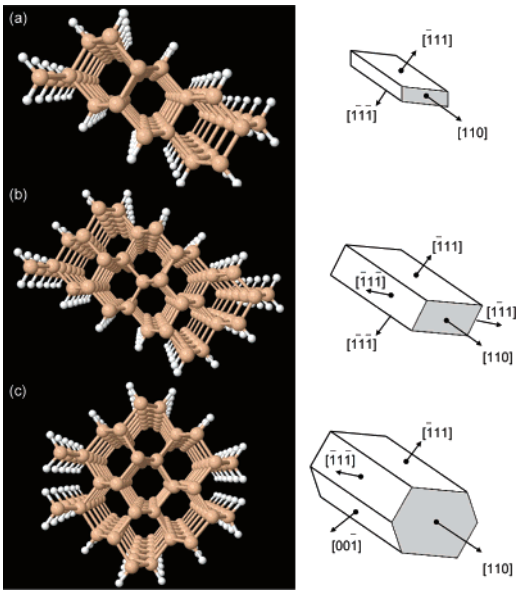

Figure 4. Magic nanowires (perspective view) found as minima of the formation energy per atom. The chain (a) and double chain (b) are characterized by the number of complete six-atom rings R and double rings D, respectively (also refer to Table 1). The configurations with hexagonal cross section have a number L of full concentric layers ($L = 2$ in panel (c) above) of six rings and are consistent with recent observations of H-passivated SiNWs.[6,7] The facet orientations of magic wires are shown on the right.

Table 1. Building Blocks and Magic Numbers (n) of Si Atoms Corresponding to the Different Types of Low-Energy SiNWs Found in the Global Optimization[a]

structure	building units	n	mono-H	di-H
chain	rings, R	$4(R+1)$	$2(R+1)$	2
double chain	double rings, D	$6(D+1)$	$2(D+2)$	2
hexagon	layers, L	$2L(3L+1)$	$4L$	$2L$

[a] The last two columns show the number of mono- and dihydrides in each case.

is not predicted by the surface energies because the interactions of facet edges are significant for wires thinner than 2 nm.

To our knowledge, chain and double-chain wires have not been observed so far for SiNWs, perhaps because the diameters achieved in the laboratory are larger than those which are favorable for platelike structures to form.[6] Recent experiments were successful in isolating and characterizing [110] SiNWs with hexagonal section and diameters between 1.3 and 7 nm.[6] The thinnest hexagonal wire in our work ($L = 2$ in Table 1) has a diameter of approximately 1.2 nm, as estimated by the distance between its {001} facets. The first hexagonal wire that we find to be more stable than any double-chain magic wire is about 1.8 nm in diameter, i.e., already in the range of the experimentally reported hexagonal SiNWs.[6] Pursuing further the comparison between the hexagonal wires found here and those in ref 6, we have computed STM images for the facets of the $L = 5$ hexagon. The simulated images are shown in Figure 6a for a {111} facet covered with monohydride and for a {001} facet covered with dihydride. Our calculations are in agreement

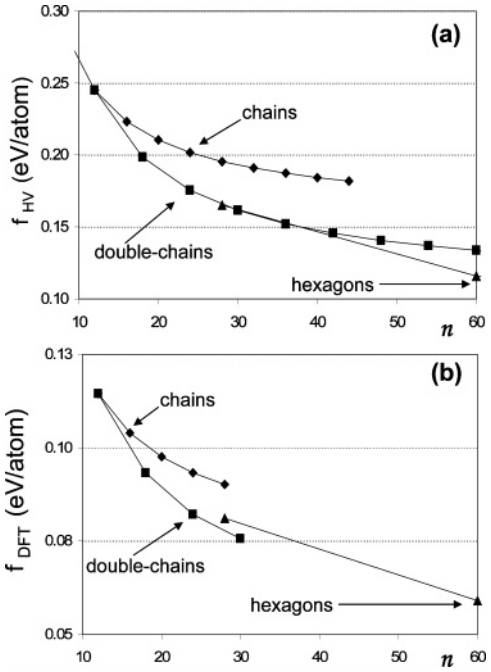

Figure 5. Formation energies per Si atom computed for specific structures of the H-passivated [110] nanowires: chain (diamonds), double chain (squares), and hexagonal (triangles up), computed at the level of HV potential[21] with $\mu_H = -2.42$ eV (a) and of DFT calculations[22] with $\mu_H = -3.45$ eV (b).

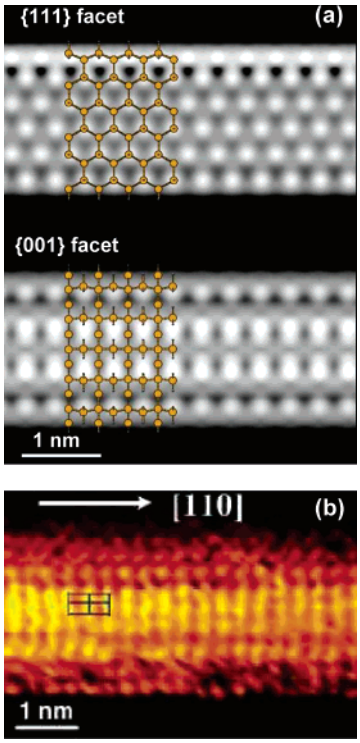

Figure 6. (a) Simulated empty-state STM images (bias of +2.0 V) of {111} and {001} facets of an $L = 5$ hexagonal nanowire. (b) Actual STM image of a {001} facet (from ref 6) taken at the same bias voltage. (Reprinted with permission from ref 6. Copyright 2003 American Association for the Advancement of Science).

with the STM experiments, which also showed the exclusive presence of dihydride species on the {001} facets of [110] SiNWs. Furthermore, the resemblance (Figure 6) between

the simulated STM image and the experimental one brings strong support to the predictive power of the theoretical methodology presented here.

In conclusion, we described a combined GA-DFT procedure to search for the structure of [110] passivated SiNWs and presented our results for [110] nanowires with up to 60 atoms per unit cell. Subject to the availability of reasonable empirical potentials, this GA-DFT procedure can be adapted quite readily for finding the structure of any type of nanowire that exhibits atomic-scale periodicity along its axis. For H-passivated [110] silicon wires, the genetic search revealed three types of magic structures (shown in Figure 4), chain, double-chain, and hexagonal SiNWs. Our results for hexagonal wires are consistent with recent experiments.[6] Given this agreement with experiments at diameters larger than 1.8 nm, it is conceivable that the chain and double-chain structures proposed here can be observed experimentally upon pursuing the preparation of SiNWs thinner than 1.3 nm.

Acknowledgment. Ames Laboratory is operated for the U.S. Department of Energy by Iowa State University under Contract No. W-7405-Eng-82. This work was supported by the Director for Energy Research, Office of Basic Energy Sciences including a grant of computer time at the National Energy Research Supercomputing Center (NERSC) in Berkeley and the EMSL computational resources at the Pacific Northwest National Laboratory.

References

(1) Appell, D. *Nature* (*London*) **2002**, *419*, 553.
(2) Cui, Y.; Lieber, C. M. *Science* **2001**, *291*, 851 .
(3) Morales, A. M.; Lieber, C. M. *Science* **1998**, *269*, 208.
(4) Zhang, R.-Q.; Lifshitz, Y.; Lee, S.-T. *Adv. Mater.* **2003**, *15*, 635.
(5) Holmes, J. D.; Johnston, K. P.; Doty, R. C.; Korgel, B. A. *Science* **2000**, *287*, 1471.
(6) Ma, D. D. D.; Lee, C. S.; Au, F. C. K.; Tong, S. Y.; Lee, S. T. *Science* **2003**, *299*, 1874.
(7) Wu, Y.; Cui, Y.; Huynh, L.; Barrelet, C. J.; Bell, D. C.; Lieber, C. M. *Nano Lett.* **2004**, *4*, 433.
(8) Schmidt, V.; Senz, S.; Gösele, U. *Nano Lett.* **2005**, *5*, 931.
(9) Menon, M.; Richter, E. *Phys. Rev. Lett* **1999**, *83*, 792.
(10) Zhao, Y.; Yakobson, B. I. *Phys. Rev. Lett.* **2003**, *91*, 035501.
(11) Bai, J.; Zeng, X. C.; Tanaka, H.; Zeng, J. Y. *Proc. Natl. Acad. Sci. U.S.A.* **2004**, *101*, 2664.
(12) Rurali, R.; Lorente, N. *Phys. Rev. Lett.* **2005**, *94*, 026805.
(13) Kagimura, R.; Nunes, R. W.; Chacham, H. *Phys. Rev. Lett.* **2005**, *95*, 115502.
(14) Cui, Y.; Gudiksen, L. J.; Wang, M. S.; Lieber, C. M. *Appl. Phys. Lett.* **2001**, *78*, 2214.
(15) Wang, N.; Tang, Y. H.; Zhang, Y. F.; Lee, C. S.; Bello, I.; Lee, S. T. *Chem. Phys. Lett.* **1999**, *299*, 237.
(16) Hanrath, T.; Korgel, B. A. *Small* **2005**, *1*, 717 .
(17) Refer to, e.g.: Pimpinelli, A.; Villain, J. *Physics of crystal growth*; Cambridge University Press: Cambridge, 1998; Chapter 3.
(18) Ho, K. M.; Shvartsburg, A. A.; Pan, B. C.; Lu, Z. Y.; Wang, C. Z.; Wacker, J.; Fye, J. L.; Jarrold, M. F. *Nature* **1998**, *392*, 582.
(19) Chuang, F. C.; Ciobanu, C. V.; Shenoy, V. B.; Wang, C. Z.; Ho, K. M. *Surf. Sci.* **2004**, *573*, L375.
(20) Chuang, F. C.; Ciobanu, C. V.; Predescu, C.; Wang, C. Z.; Ho, K. M. *Surf. Sci.* **2005**, *578*, 183.
(21) Hansen, U.; Vogl, P. *Phys. Rev. B* **1998**, *57*, 13295.
(22) VIENNA ab initio simulation package, Technische Universität Wien, 1999; Kresse, G.; Hafner, J. *Phys. Rev. B* **1993**, *47*, R558; Kresse, G.; Furthmuller, J. *Phys. Rev. B* **1996**, *54*, 11169.
(23) The ab initio calculations are performed within the generalized gradient approximation.[24] The kinetic energy cutoff is set at 11 Ry, and the Brillouin zone is sampled using 16 *k* points. The SiNW is positioned at the center of a supercell with a vacuum space of 12 Å separating the periodic images of the wires. Each SiNW structure is relaxed until the magnitude of the force on any atom is smaller than 0.01 eV/Å.
(24) Perdew, J. P. In *Electronic Structure of Solids '91*; Ziesche, P., Eschrig, H., Eds.; Akademie-Verlag: Berlin, 1991.
(25) Zhao, X.; Wei, C. M.; Yang, L.; Chou, M. Y. *Phys. Rev. Lett.* **2004**, *92*, 236805.

NL0522633